# Structure of Cationized Arginine (Arg·$M^+$, M = H, Li, Na, K, Rb, and Cs) in the Gas Phase: Further Evidence for Zwitterionic Arginine

**Rebecca A. Jockusch, William D. Price, and Evan R. Williams***

*Department of Chemistry, University of California, Berkeley, California 94720-1460*

*Received: September 3, 1999*

The gas-phase structures of cationized arginine, Arg·$M^+$, M = Li, Na, K, Rb, and Cs, were studied both by hybrid method density functional theory calculations and experimentally using low-energy collisionally activated and thermal radiative dissociation. Calculations at the B3LYP/LACVP++** level of theory show that the salt-bridge structures in which the arginine is a zwitterion (protonated side chain, deprotonated C-terminus) become more stable than the charge-solvated structures with increasing metal ion size. The difference in energy between the most stable charge-solvated structure and salt-bridge structure of Arg·$M^+$ increases from −0.7 kcal/mol for Arg·$Li^+$ to +3.3 kcal/mol for Arg·$Cs^+$. The stabilities of the salt-bridge and charge-solvated structures reverse between M = Li and Na. These calculations are in good agreement with the results of dissociation experiments. The low-energy dissociation pathways depend on the cation size. Arginine complexed with small cations (Li and Na) loses $H_2O$, while arginine complexed with larger cations (K, Rb, and Cs) loses $NH_3$. Loss of $H_2O$ must come from a charge-solvated ion, whereas the loss of $NH_3$ can come from the protonated side chain of a salt-bridge structure. The results of dissociation experiments using several cationized arginine derivatives are consistent with the existence of these two distinct structures. In particular, arginine methyl esters, which cannot form salt bridges, dissociate by loss of methanol, analogous to loss of $H_2O$ from Arg·$M^+$; no loss of $NH_3$ is observed. Although dissociation experiments probe gas-phase structure indirectly, the observed fragmentation pathways are in good agreement with the calculated lowest energy isomers. The combination of the results from experiment and theory provides strong evidence that the structure of arginine−alkali metal ion complexes in the gas phase changes from a charge-solvated structure to a salt-bridge structure as the size of the metal ion increases.

## Introduction

Zwitterions and salt bridges are ubiquitous in biological molecules where they are of great functional and structural significance. In water at neutral pH, single amino acid residues and oligopeptides exist as zwitterions in which the N-terminus is protonated and the C-terminus is deprotonated. Additional charges occur on residues with acidic or basic side chains. These charge-separated species are stabilized in vivo by multiple interactions with solvent molecules. The stability of zwitterions in the absence of solvent has been the subject of many theoretical[1−8] and experimental[9−16] investigations. Numerous studies have shown that the simplest amino acid, glycine, is not a zwitterion in the gas phase.[1−6,9−11] However, calculations show that the glycine zwitterion may be stabilized by as few as one[5] or two[6] water molecules. The side chain of arginine is significantly more basic than the N-terminus. This should stabilize the arginine zwitterion relative to the simple neutral structure. Calculations using density functional theory with modest size basis sets indicate that the stability of the zwitterion structure of isolated arginine in which the side chain is protonated is comparable with the nonzwitterion form.[12] However, recent results from IR cavity ringdown spectroscopy experiments indicate that the nonzwitterion form is more stable.[13] The zwitterion form can be stabilized by the presence of an additional charge, thereby forming a salt bridge. Recent experimental results indicate that the proton-bound dimer of arginine is a salt bridge in which one of the arginine molecules exists as a zwitterion.[12]

There is now significant evidence that salt bridges play a role in the chemistry of gas-phase biomolecule ions.[17−29] For example, the most stable form of protonated bradykinin, a nine residue peptide, is one in which both terminal arginine residues are protonated and the C-terminus is deprotonated.[17] The salt bridge is stabilized intramolecularly by interactions with carbonyl oxygens of the peptide backbone. Mechanisms involving stable salt-bridge structures have also been proposed[18,19] to explain the facile cleavages seen after acidic residues in peptides and proteins[20−22] as well as fragmentations promoted by alkali metal ion binding of peptides.[22−24]

Larger peptides are sufficiently flexible that intramolecular solvation can help stabilize a salt bridge. The intramolecular solvation occurs mostly through interactions of the charged groups with polar groups in the molecule, primarily the carbonyl oxygens of the oligopeptide backbone. These interactions provide a near equivalent to a "solvent shell" around the charge. The question remains as to how stable salt-bridge structures are in smaller ions, such as amino acids, which have little or no self-solvating ability. Calculations on glycine−alkali metal ion complexes indicate that the salt-bridge structure is higher in energy than the most stable charge-solvated (nonsalt-bridge) form by only 1−4 kcal/mol.[7,8] Results from ion mobility experiments on sodiated glycine show that these ions exist in the charge-solvated form.[14]

* To whom correspondence should be addressed.

10.1021/jp9931307 CCC: $18.00 
Published on Web 11/03/1999

Very recently, the results of ion mobility studies of protonated, sodiated, and cesiated arginine have been reported.[30] Single peaks were observed in the arrival time distributions of each Arg·$M^+$ at 300 K, indicating the presence of one or more structures with the same cross section or several structures that rapidly interconvert. The measured cross sections of each Arg·$M^+$ are consistent with the range of cross sections calculated for both the charge-solvated and salt-bridge forms of these ions. Thus, no definitive conclusions about the structure of these ions could be deduced from these experiments. Ab initio calculations on a similar but smaller molecule, sodiated *N*-amidinoglycine (NAG), indicate that the salt-bridge form is more stable than the charge-solvated form, but the ion mobility experiments were more consistent with a charge-solvated form. The authors stated that "at this point, no definitive conclusion can be made about the structure of [NAG]$Na^+$."

Here, we present evidence that the structure of arginine−alkali metal ion complexes (Arg·$M^+$), M = H, Li, Na, K, Rb, and Cs, depends on the size of the cation. For M = H and Li, the gas-phase complex appears to exist predominantly as a charge-solvated (nonzwitterion) structure, whereas for M = K, Rb, and Cs, the structure is a salt bridge. These conclusions are based on the results of dissociation experiments using both thermal radiation and collisional activation techniques as well as hybrid method density functional theory (DFT) calculations. For M = Na, experimental results indicate that the charge-solvated form is favored, whereas the calculations indicate that the salt-bridge form is favored. The DFT calculations show a clear trend that salt-bridge structures become more stable relative to the charge-solvated structures as the metal ion size increases.

## Experimental Section

**Mass Spectrometry.** All experiments were performed on a home-built Fourier-transform mass spectrometer which has a 2.7 T superconducting magnet. The instrumentation has been described in detail elsewhere.[31] Protonated ions are formed by electrospray ionization. The ions are guided through five stages of differential pumping into the ion cell where they are trapped. A pulse of nitrogen gas at a pressure of $2 \times 10^{-6}$ Torr is used during ion accumulation to assist in trapping and thermalization of the ions. The base pressure of the cell at other times is less than $3 \times 10^{-8}$ Torr. The ion accumulation time is varied between 1 and 10 s to optimize ion signal. After the ion accumulation event, a shutter is closed to prevent additional ions from entering the cell. The complexes are isolated using a series of stored waveform inverse Fourier transform, chirp, and single frequency excitation waveforms. For the blackbody infrared radiative dissociation (BIRD) experiments, complexes are stored inside the vacuum chamber which is heated to temperatures between 180 and 206 °C. The complexes are allowed to dissociate for times up to 300 s. For the sustained off-resonance irradiation collisionally activated dissociation (SORI−CAD) experiments, a RF waveform ($1.6V_{p-p}$ for M = Li, Na, K, Rb, and Cs; $2.4-2.7V_{p-p}$ for M = H) with a frequency corresponding to 1.0 mass-to-charge unit below that of the isolated molecular ion is applied for a duration of 1 s. Nitrogen is used as the collision gas in the SORI−CAD experiments. These conditions correspond to maximum center-of-mass collision energies ranging from 0.24 to 1.11 eV. A broad-band excitation rf chirp at a sweep rate of 3200 Hz/$\mu$s was used to excite the ions for detection. A Finnigan Odyssey data system (Madison, WI) was used to collect the data at an acquisition rate of 2286 kHz (*m*/*z* 36 cutoff) for all complexes. For ions containing $Na^+$, additional data sets using an acquisition rate of 5333 kHz (*m*/*z* 15 cutoff) were collected.

**SCHEME 1**

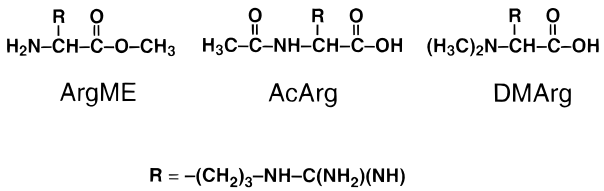


Arginine (Arg), *N*,*N*-dimethylarginine (DMArg), and *N*-acetylarginine (AcArg) (Scheme 1) were purchased from Sigma Chemical Co. (St. Louis, MO) and were used without further purification. Arginine methyl ester (ArgME) was synthesized by adding a drop of concentrated sulfuric acid to a $\sim 10^{-4}$ M solution of arginine in methanol and allowing the mixture to sit overnight. Metal complexes were formed in solution by mixing a concentrated solution of the metal acetate salt in water into $\sim 10^{-4}$ M methanol solutions of Arg, DMArg, AcArg, and ArgME in ratios which optimized the amount of metal−arginine (or Arg derivative) complex formed.

**Computational Methods.** Three isomers of the arginine−alkali metal ion complexes (Arg·$M^+$) were built using the Insight/Discover package (Biosym Technologies, San Diego, CA) for each M = Li, Na, K, Rb, and Cs. In one of these isomers, the arginine is a zwitterion (protonated guanidino group of the side chain and deprotonated carboxylate group at the C-terminus). With the addition of a metal ion, the complex becomes a salt bridge and is termed SB. In the remaining two isomers, the arginine is not a zwitterion; instead the guanidino group of the side chain is not protonated, and the C-terminus is a carboxyl (COOH) group. The site of deprotonation of the guanidino group distinguishes these two isomers. With the addition of a metal ion to these nonzwitterionic arginine structures, these are called the "charge-solvated" (ChS) complexes.

An ensemble of low-energy conformations of each of the three isomeric complexes was generated through molecular dynamics simulations using the AMBER force field provided with the Discover package. For the SB structures, dynamics were carried out at 900 K for 5 ps. The ChS structure dynamics were run for 5 ps at 700 K for M = Li and Na, at 600 K for M = K and Rb, and at 400 K for M = Cs. This was followed by simulated annealing to 200 K over an additional 5 ps. Each conformer was subsequently energy minimized. The energy minimized conformer was archived and used as the starting geometry for a new dynamics simulation. A total of 120 structures for each isomer were generated following this procedure. All archived structures within 5 kcal/mol were examined to find starting structures for higher level geometry optimization and energy calculations. The archived structures were classified into families according to intramolecular arginine interactions and arginine−metal ion interactions. The potential energy surfaces for these complexes have many minima and are quite complicated. Thus, families of structures selected represent only a subset of possible structures. Often, several structures with similar number and types of interactions were found. To choose among these, the structures were optimized at a higher level, and if they optimized to different geometries, the most stable structure was selected. In this fashion, a total of seven families of structures, three different families of salt-bridge structures and two families of each of the charge-solvated structures, were selected to optimize for each Arg·$M^+$ at a higher level of theory.

The hybrid method B3LYP was used for geometry optimization and energy evaluation of each of the seven families of

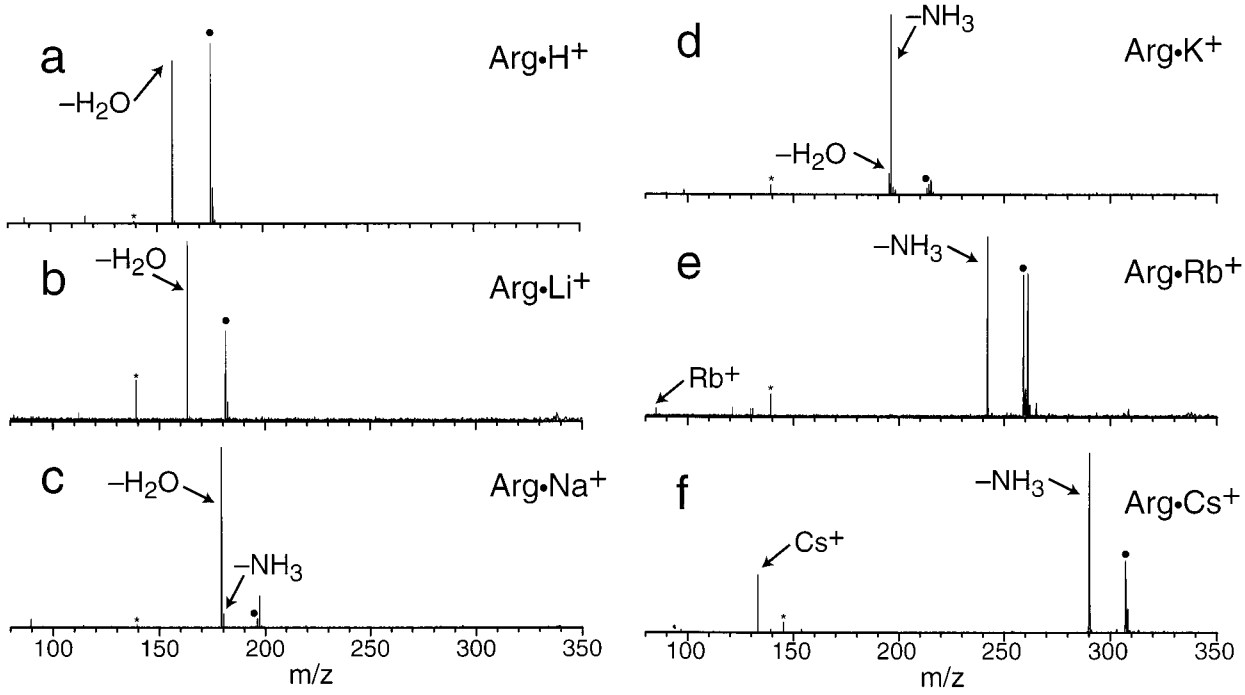


**Figure 1.** Low-energy collisionally activated dissociation spectra of Arg•$M^+$, M = H, Li, Na, K, Rb, and Cs. The isotopic distribution of the complex is isolated, but the lowest *m/z* isotope is preferentially excited and dissociated under the conditions of the experiment. The parent ion is indicated by a (●) in each spectrum. (*) indicates frequency noise.

structures selected from dynamics simulations. These calculations were done using Jaguar v. 3.0 and 3.5 (Schrodinger, Inc., Portland, OR) on a DEC alpha 500 AU workstation. The basis set used in these calculations is LACVP** which is a basis set of double-ζ quality incorporating an effective core potential of Hay and Wadt[32] for the K, Rb, and Cs metals and using the 6-31G** basis set for the other atoms. The starting geometry used for the first Arg•$M^+$ calculated for any family was from dynamics. Subsequent calculations used the B3LYP/LACVP** geometry for an M of neighboring size as the starting point. For example, the salt-bridge conformer selected from dynamics for Arg•$K^+$ was optimized at the B3LYP/LACVP** level. This optimized geometry was then used as a starting structure for Arg•$Na^+$ and Arg•$Rb^+$ of the same salt-bridge family, and so on. In addition to the 35 structures reported in this paper, geometry optimizations on over 30 other structures were performed at the B3LYP/LACVP** level in the course of selecting the seven families of structures for optimization with all M's. Thus, although results from only a subset of possible structures are reported, these structures should represent the more stable salt-bridge and charge-solvated structures of the Arg•$M^+$ complexes.

Higher level calculations using larger basis sets were performed using Jaguar v. 3.5 and GAUSSIAN 92/DFT (Gaussian Inc., Pittsburgh, PA) on the lowest energy LACVP** charge-solvated and salt-bridge structures. After reoptimization, frequencies for the lowest energy charge-solvated and salt-bridge structures were calculated at the RHF/3-21G level for all metalated arginine ions except Cs for which the basis set is not available. Structures at this level were very similar to the B3LYP geometries. The frequencies are all real and were used to calculate zero-point energies after scaling by 0.90.[33]

## Results and Discussion

**Dissociation of Arg•$M^+$.** Figure 1 shows the results of collisionally dissociating Arg•$M^+$, M = H, Li, Na, K, Rb, and Cs using sustained off-resonance irradiation collisionally activated dissociation (SORI−CAD). With SORI−CAD, ions are subject to rf radiation slightly off-resonance from their cyclotron frequency. Ions undergo periodic acceleration/deceleration cycles during which collisional activation at low energy occurs. In all experiments, the entire isotopic distribution of the precursor ions was isolated. The frequency of the SORI waveform is higher (lower *m/z*) than the cyclotron frequency of the ions. This results in preferential excitation and dissociation of the lowest *m/z* ion in the isotopic cluster. Using SORI−CAD, Arg•$H^+$ and Arg•$Li^+$ dissociate exclusively by loss of $H_2O$ (parts a and b of Figure 1). Arg•$Na^+$ dissociates predominantly by loss of $H_2O$; a small amount of loss of $NH_3$ is observed (Figure 1c). For Arg•$K^+$, the relative abundances of these two losses is reversed (Figure 1d); the major fragment corresponds to a loss of $NH_3$, and a small amount of loss of $H_2O$ is observed. No metal ion ejection is observed from either Arg•$Na^+$ or Arg•$K^+$. Arg•$Rb^+$ and Arg•$Cs^+$ dissociate primarily by loss of $NH_3$ with some $Rb^+$ and $Cs^+$ observed. No loss of $H_2O$ is seen for either of these larger metal ions. Dissociation spectra obtained using blackbody infrared radiative dissociation (BIRD) show the same fragmentation products as the SORI−CAD results. In the BIRD technique, the entire vacuum chamber is heated to a uniform temperature, and the ions are activated by direct absorption of photons emitted by the vacuum chamber walls.

These results clearly show that the fragmentation observed under low-energy dissociation conditions depends strongly on the size of the metal ion. Protonated arginine and arginine complexed with small metal ions fragment by loss of $H_2O$; arginine complexed with large metals fragment by loss of $NH_3$ with some metal ion ejection also observed. The cross over between loss of $H_2O$ and $NH_3$ is between Arg•$Na^+$ and Arg•$K^+$. These data are summarized in Table 1. The results suggest that the gas-phase structure of the Arg•$M^+$ complex is different for small and large M.

The loss of $H_2O$ must come from the C-terminus, as this is the location of the only oxygens in the Arg•$M^+$ ions. It is difficult to rationalize how a loss of $H_2O$ could come from a

**TABLE 1: Fragmentations Observed from Cationized Arginine and Arginine Derivatives from Both Thermal Radiation and Collisional Activation Dissociation Experiments (Most Abundant Fragment Indicated by Bold Type)**

| M | Arg·$M^+$ | ArgME·$M^+$ | DMArg·$M^+$ | AcArg·$M^+$ |
|---|---|---|---|---|
| H | −**$H_2O$** | −**$CH_3OH$** | −**$H_2O$**, $-NH_3$, −45 | −**$H_2O$**, $-NH_3$, −60 |
| Li | −**$H_2O$** | −**$CH_3OH$** | −**$H_2O$** | −**$H_2O$**, −60 |
| Na | −**$H_2O$**, $-NH_3$ | −**$CH_3OH$** | −**$H_2O$** | −**$H_2O$** |
| K | $-H_2O$, −**$NH_3$** | −**$CH_3OH$**, $K^+$ | −**$H_2O$**, $-NH_3$, $K^+$, −45 | −**$H_2O$**, −60 |
| Rb | −**$NH_3$**, $Rb^+$ | $-CH_3OH$, **$Rb^+$** | −**$H_2O$**, $-NH_3$, $Rb^+$, −45 | −**$H_2O$**, −60 |
| Cs | −**$NH_3$**, $Cs^+$ | $-CH_3OH$, **$Cs^+$** | $-H_2O$, $-NH_3$, **$Cs^+$**, −45 | **$Cs^+$** |

**SCHEME 2**

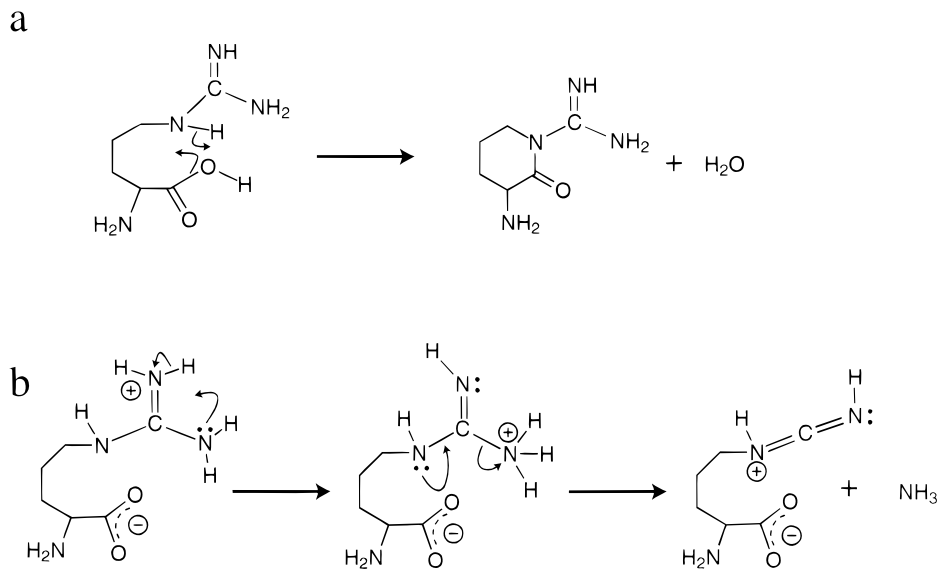


salt-bridge structure. The first step of the mechanism for this loss would have to be the protonation of the carboxylate, thus destroying the zwitterionic character of the arginine and hence the salt bridge. On the other hand, loss of $NH_3$ can readily come from a salt-bridge structure. Scheme 2 shows simple mechanisms which have been proposed for the loss of $H_2O$ from a charge-solvated structure and loss of $NH_3$ from the protonated guanidino group of the arginine side chain.[25] In both these mechanisms, as well as in several others that can be drawn for these losses, a hydrogen migration is necessary prior to dissociation. While the loss of $H_2O$ is suggestive of a nonzwitterionic form and the loss of $NH_3$ is suggestive of a zwitterionic form of arginine, these dissociation pathways are indirect evidence of equilibrium structure. Isomerization of the structures can occur prior to the observed fragmentation. To the extent that the transition state entropy for dissociation by these two pathways is similar (both are simple rearrangement reactions), then the change in fragmentation of Arg·$M^+$ from loss of $H_2O$ for M = H to Na to loss of $NH_3$ for M = K to Cs suggests that the complex changes from a charge-solvated species with the small metal ions ($Li^+$, $Na^+$) to a salt-bridge species with the larger metal ions ($K^+$, $Rb^+$, $Cs^+$). Another possible explanation is that these ions all have one structure or isomerize prior to the observed fragmentation but that the relative fragmentation activation energy or entropy for these two processes change as a function of cation size. To distinguish between these possible explanations, additional dissociation experiments were performed on several series of arginine derivative−cation complexes.

**Dissociation of Arg-Derivatives·$M^+$.** Cationized arginine methyl esters (ArgME·$M^+$) cannot form salt-bridge structures. Dissociation of the protonated and all metalated species, ArgME·$M^+$, using both SORI−CAD and BIRD results in neutral loss of 32. This corresponds to a loss of $CH_3OH$, i.e., loss of the derivatized C-terminus, analogous to loss of $H_2O$ from Arg·$M^+$. The larger metalated species, ArgME·$Cs^+$, ArgME·$Rb^+$, and to some extent ArgME·$K^+$, also dissociate by metal ion ejection. No loss of $NH_3$ was observed for any of the ArgME·$M^+$ species. The absence of the $NH_3$ loss pathway for the larger metal ions is consistent with a charge-solvated structure for these methyl esters.

To investigate the origin of the loss of $NH_3$, two series of N-terminally derivatized arginine−cation complexes were dissociated. SORI−CAD spectra of protonated and metalated *N,N*-dimethylarginine (DMArg·$M^+$) are shown in Figure 2. Loss of $H_2O$ is observed for both M = Li and Na (parts b and c of Figure 2). DMArg·$K^+$ dissociates primarily by loss of $H_2O$, but a small amount of $NH_3$ loss is observed (Figure 2d). For the larger metals, water loss decreases and the loss of $NH_3$ increases. Roughly equal amounts of $NH_3$ and $H_2O$ loss are observed in the SORI−CAD spectrum of DMArg·$Cs^+$ (Figure 2f). Similar results are obtained from BIRD experiments. The change in fragmentation pathways with increasing metal ion size is similar to the pattern observed for Arg·$M^+$, except that the cross over point (defined as the point where fragments corresponding to losses of $NH_3$ and $H_2O$ are equal in abundance) for the DMArg·$M^+$ species is at M = Cs compared to between M = Na and M = K for the Arg·$M^+$ species. In addition to the losses of $NH_3$ and $H_2O$, some loss of 45 (presumably loss of dimethylamine from the N-terminus) as well as ejection of $M^+$ is observed for M = K, Rb, and Cs. In this series of experiments, the loss of $NH_3$ must occur from the side chain, not the (derivatized) N-terminus. This indicates that it is possible for Arg·$M^+$ to lose $NH_3$ from the arginine side chain.

The fragment ion corresponding to the loss of 45 from the DMArg·$M^+$ species is similar in abundance to the fragment ion corresponding to the loss of $NH_3$. This may mean that some or even all of the loss of $NH_3$ could possibly occur from the

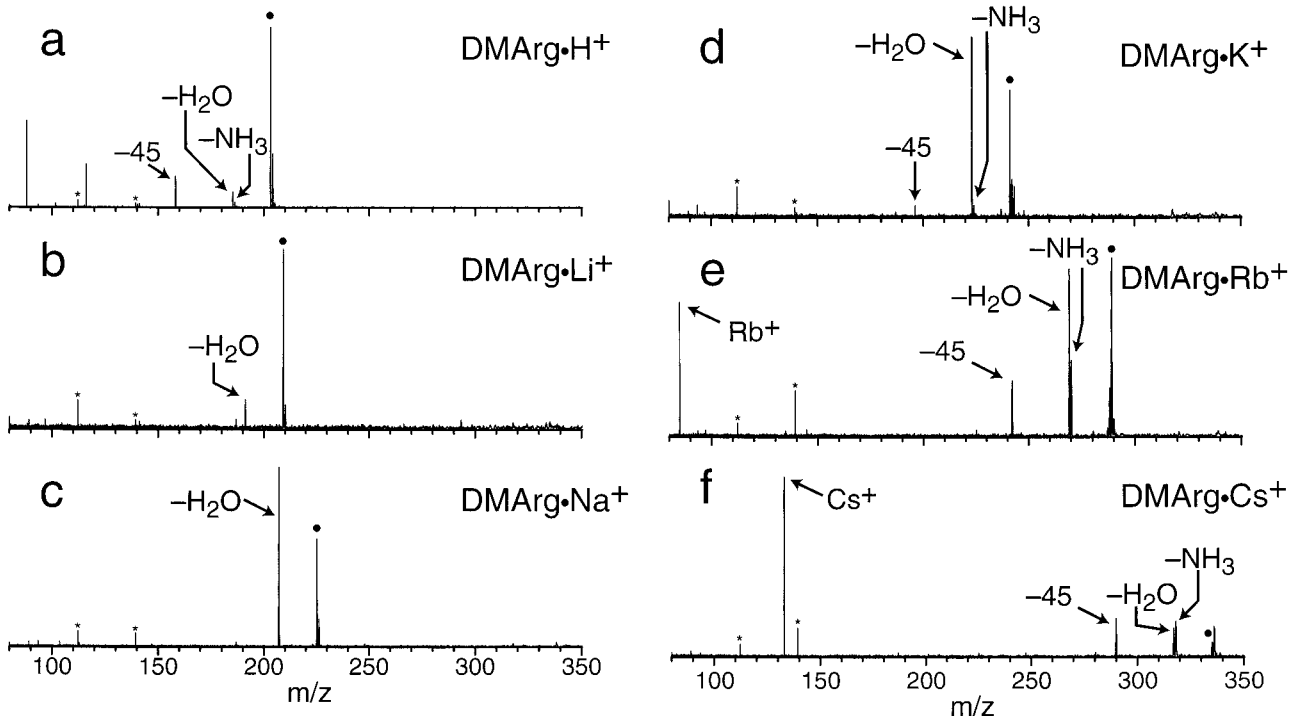


**Figure 2.** Low-energy collisionally activated dissociation spectra of cationized *n,n*-dimethylarginine (DMArg•$M^+$). The parent ion is indicated by a (●) in each spectrum. (*) indicates frequency noise.

N-terminus in Arg•$M^+$. Protonation of the N-terminus seems less likely since the gas-phase basicity of the N-terminus of amino acids is lower than that of the guanidino group of the side chain by ~20 kcal/mol[34] making it energetically much less favored. However, we cannot rule out this possibility.

The dissociation of *N*-acetylarginine complexes (AcArg•$M^+$) was also investigated. For M = Li, Na, and K, the primary dissociation pathway was loss of $H_2O$. For M = Rb and Cs, the primary fragment was $M^+$, although some loss of $H_2O$ was observed from AcArg•$Rb^+$. SORI−CAD spectra also showed a loss of 60. This loss has previously been assigned to the loss of $H_2O$ followed by loss of HN=C=NH due to a rearrangement of the arginine side chain in peptides containing C-terminal arginine residues.[23,25] No loss of $NH_3$ was observed in either the BIRD or SORI−CAD spectra for any of the metalated species of AcArg. The loss of $H_2O$ that is seen for all M is consistent with AcArg•$M^+$ being a charge-solvated structure. The additional carbonyl of the acetyl group ($H_3CCO$−) is expected to increase the solvating ability of AcArg compared to Arg which apparently results in greater stabilization of the charge-solvated complex.

Interestingly, both DMArg•$H^+$ and AcArg•$H^+$ require a great deal more energy to dissociate than any of the metalated species. DMArg•$H^+$ showed no fragmentation using BIRD at 195 °C with a 100 s reaction delay compared to greater than 88% dissociation for all metalated species under the same conditions. The SORI−CAD spectrum obtained for DMArg•$H^+$ shows some loss of $H_2O$ and 45 as well as a small amount of $NH_3$ loss (Figure 2a), similar to DMArg complexed with the larger cations. However, the major fragments seen are at *m/z* 88 and 116 which are not observed from any of the metalated species. These fragments most likely correspond to cleavage between the $\beta$ and $\gamma$ carbons of the arginine side chain. AcArg•$H^+$ is also thermally stable in comparison to the metalated species and could not be dissociated using BIRD. A SORI−CAD spectrum of AcArg•$H^+$ (using a maximum center-of-mass collision energy of 1.1 V compared to 0.4−1.0 V for the metalated species) shows a similar fragmentation pattern to the metalated species. Some loss of $NH_3$ as well as $H_2O$ is observed, although loss of 60, corresponding to a loss of water followed by a rearrangement reaction and loss of part of the side chain,[23,25] is the major fragment. The much greater dissociation energy required for all the protonated species and the greater number of fragmentation channels observed make it difficult to draw structural comparisons to the metalated species.

**Fragmentation Efficiencies.** Figure 3 shows BIRD dissociation spectra for Arg•$K^+$, ArgME•$K^+$, DMArg•$K^+$, and AcArg•$K^+$ measured at a cell temperature of 200 °C. Parts a−c of Figure 3 are taken after a reaction delay of 30 s. Figure 3d (AcArg•$K^+$) has a reaction delay of 100 s. These complexes should have similar IR absorption rates due to their structural similarities. Thus, the relative fragmentation efficiency should be a rough indication of the accessibility of the corresponding dissociation pathway for a given complex. After 30 s at 200 °C, Arg•$K^+$ is ~80% dissociated. The main fragment ion is loss of $NH_3$ (~85%), with some loss of $H_2O$ (~15%, Figure 3a). After the same reaction delay, ArgME•$K^+$ is only ~10% dissociated (loss of $CH_3OH$ is the only product). The greater stability of ArgME•$K^+$ compared to Arg•$K^+$ indicates that loss of $CH_3OH$ *is not an intrinsically low-energy process*. Rather, the pathway for loss of $NH_3$ is shut down, consistent with a change from a salt-bridge to a charge-solvated structure upon formation of the methyl ester. This result indicates that the change in fragmentation pathways with increasing cation size is due to a change in structure and not simply an effect of changes in the relative transition state barrier heights with cation size.

The fragmentation efficiency of DMArg•$K^+$ (Figure 3c) is similar to that of Arg•$K^+$ and is significantly greater than that of AcArg•$K^+$. After 30 s, DMArg•$K^+$ is over 80% dissociated (Figure 3c) while AcArg•$K^+$ is <3% dissociated (not shown). After 100 s, AcArg•$K^+$ shows only 10% dissociation (Figure 3d). Similar relative fragmentation efficiencies of DMArg•$M^+$ and AcArg•$M^+$ are obtained for M = Na to Cs by both SORI−

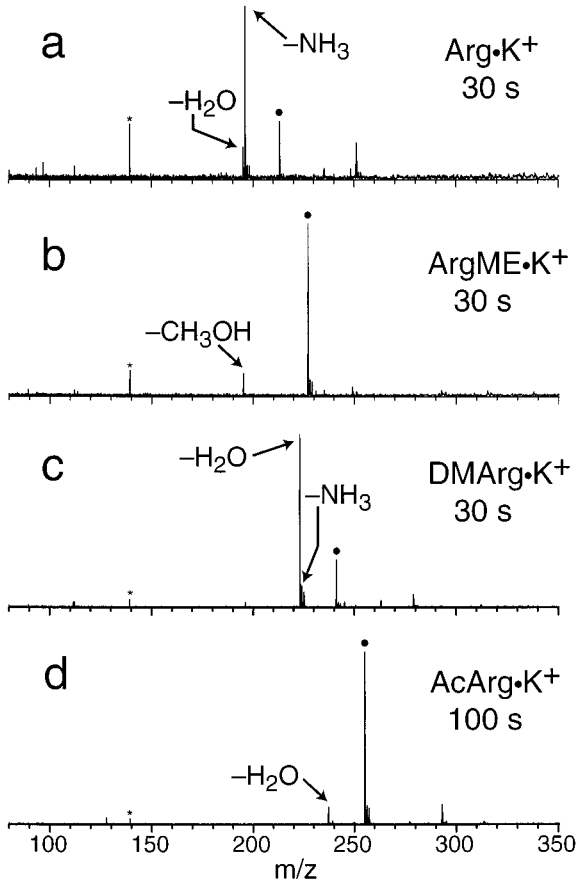


**Figure 3.** Blackbody infrared radiative dissociation spectra of potassium ion complexed with (a) arginine, (b) arginine methyl ester, (c) *n,n*-dimethylarginine, and (d) *n*-acetylarginine. All spectra were obtained at 200 °C with a 30 s (a−c) or a 100 s (d) reaction delay. (*) indicates frequency noise.

CAD and BIRD. The low fragmentation efficiency of AcArg·$K^+$ supports the explanation that acetylation of the N-terminus increases the charge solvation, thus stabilizing the ion.

**Experimental Summary.** The abrupt change in fragmentation pathways from loss of $H_2O$ to loss of $NH_3$ with increasing alkali metal ion size is remarkable. A critical question in these dissociation experiments is whether the fragment ions corresponding to loss of $H_2O$ or to loss of $NH_3$ reflect an equilibrium ion population, or whether the ions isomerize to alternate structures during the activation process. If the latter occurs, these fragment ions would not necessarily be characteristic of the equilibrium population at room temperatures. It is also possible that the relative transition state barriers for these processes reverse with increasing alkali metal ion size. The experiments with ArgME·$M^+$ suggest that this is not the case. However, we are not able to definitively distinguish between these possibilities by these experiments alone. For this reason, the relative energies of the structures were investigated computationally.

**Calculations.** The energy of three salt-bridge structures (SB1−3) and four charge-solvated structures (ChS1−4) as well as more than 30 additional structures were evaluated for Arg·$M^+$, M = Li, Na, K, Rb, and Cs at the B3LYP/LACVP** level of theory. The seven families of structures presented here were selected to represent the range of low-energy salt-bridge and charge-solvated conformations that the Arg·$M^+$ complexes may adopt. For example, out of 120 structures archived for Arg·$K^+$ from each dynamics simulation, one charge-solvated isomer had 67 different conformers that were within 5 kcal/mol of the lowest energy conformer. The other charge-solvated isomer had 66 unique conformers, and the salt-bridge isomer had 23 unique conformers within this range. It was not feasible to do higher level calculations on all the low-energy conformations generated from the dynamics simulations. The seven structures chosen as starting geometries for each series of Arg·$M^+$ B3LYP calculations represent the lowest energy geometry found within each of the seven families. The structures selected should be representative of the lower energy conformations. In particular, the more limited variety and number of different low-energy salt-bridge structures generated by dynamics (e.g., 23 versus 123 for the charge-solvated isomers of Arg·$K^+$) made it possible to more thoroughly explore the possible conformations of these complexes.

The B3LYP/LACVP** geometry optimized structures for each of the seven families of Arg·$K^+$ evaluated are shown in Figure 4. The salt-bridge structures differ from each other by whether the N-terminus points in toward the pocket formed by the arginine and helps solvate the side-chain guanidino group (SB1) or points out of the pocket and solvates the carboxylate (SB2) or the metal ion (SB3). The guanidino group at the end of the arginine side chain is protonated in aqueous solution at pH < 12.5. In the charge-solvated form, the arginine is not a zwitterion and the side chain is not protonated. There are two possible sites of deprotonation. Calculations were performed on both isomers. The guanidino groups of structures ChS1 and ChS2 are deprotonated at one of the terminal nitrogens [side chain modeled as $-(CH_2)_4NH-C(NH_2)(NH)$], while structures ChS3 and ChS4 are deprotonated at the internal nitrogen of the side chain [side chain modeled as $-(CH_2)_4N{=}C(NH_2)(NH_2)$]. Energies of four families of charge-solvated structures, consisting of two conformers of each isomer, were calculated. The N-terminus of ChS1 and ChS3 points into the pocket formed by the arginine and helps solvate the metal ion. The N-terminus of ChS2 and ChS4 points out of the pocket and forms a hydrogen bond with the acidic hydrogen of the C-terminus.

**Trends in Stability.** The conformation of the arginine in SB1 does not change significantly with cation size due to the two intramolecular hydrogen bonds; thus, the energy of this conformer is chosen as a reference for each of the Arg·$M^+$ structures. The difference in energy between the structures with SB1 taken as the zero in energy (solid line) for each Arg·$M^+$ is shown in Figure 5. From this figure, it is apparent that the charge-solvated forms in which the side chain guanidino group is modeled as $-(CH_2)_4N{=}C(NH_2)(NH_2)$ (ChS3 and ChS4) are all higher in energy than the similar structures in which the side chain is modeled as $-(CH_2)_4NH-C(NH_2)(NH)$ (ChS1 and ChS2), so only conformations of the latter charge-solvated isomer will be compared to the salt-bridge structures.

The major trend apparent from Figure 5 is that the stability of the salt-bridge structures increases relative to the charge-solvated forms as the metal ion size increases. In fact, for Arg·$K^+$, Arg·$Rb^+$, and Arg·$Cs^+$, all three of the salt-bridge structures modeled are more stable than the charge-solvated structures.

Further calculations were performed on the lowest energy charge-solvated and salt-bridge structure for each of the Arg·$M^+$. Frequencies for the lowest energy charge-solvated and salt-bridge structure for each of the metalated arginine ions except Cs were calculated at the RHF/3-21G level. This basis set is not available for Cs. The calculated frequencies were all real, confirming that each of these structures is a minimum on the potential energy surface. The frequencies were scaled by 0.90[33] and were used to calculate zero-point energies for each of the

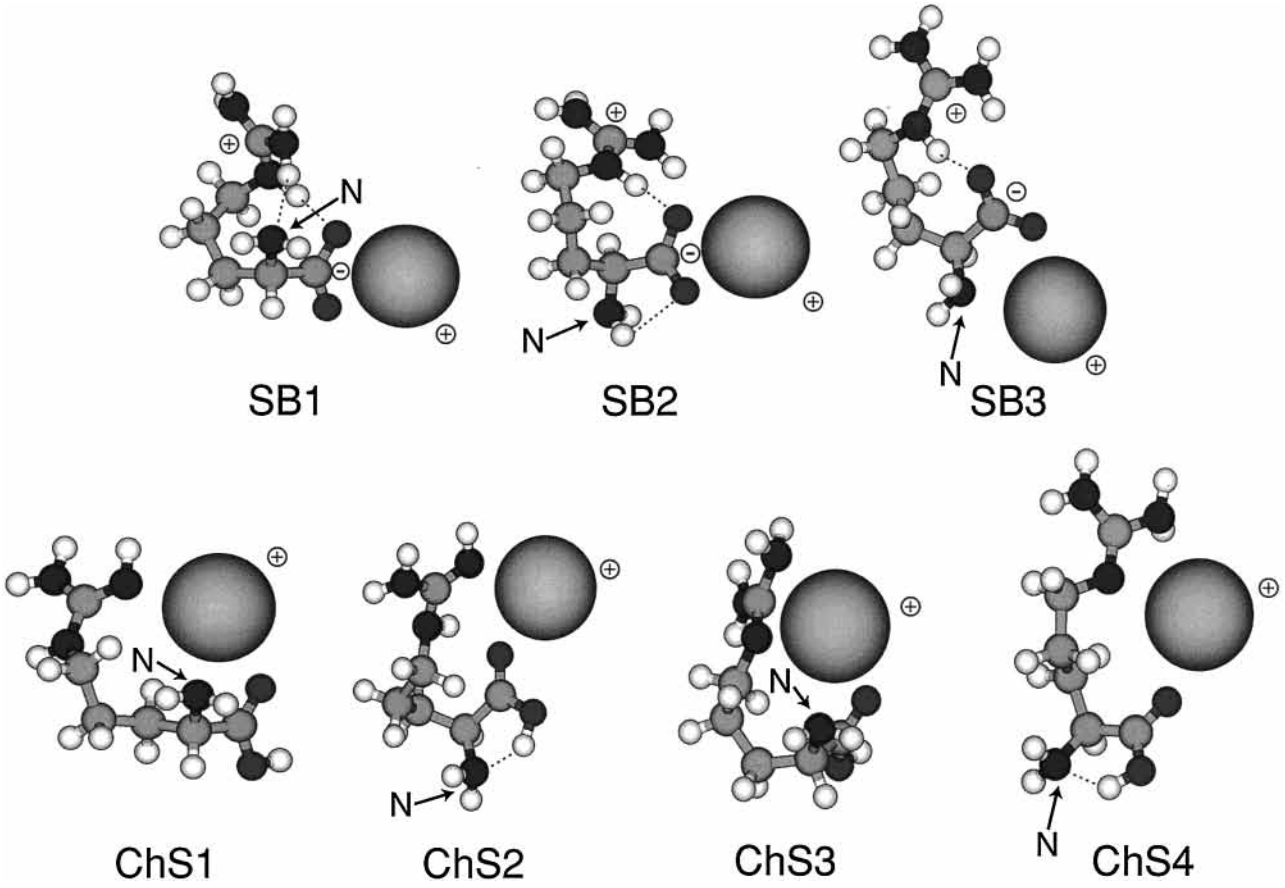


**Figure 4.** The seven families of structures obtained from molecular dynamics and selected for higher level calculations. The structures shown are the B3LYP/LACVP** geometry optimized structures for Arg·$K^+$. The structures labeled SB and ChS are salt-bridge and charge-solvated structures, respectively. The guanidino group of the Arg side chain of ChS1 and ChS2 is deprotonated at a terminal nitrogen, whereas the ChS3 and ChS4 are deprotonated at the internal nitrogen of the side chain.

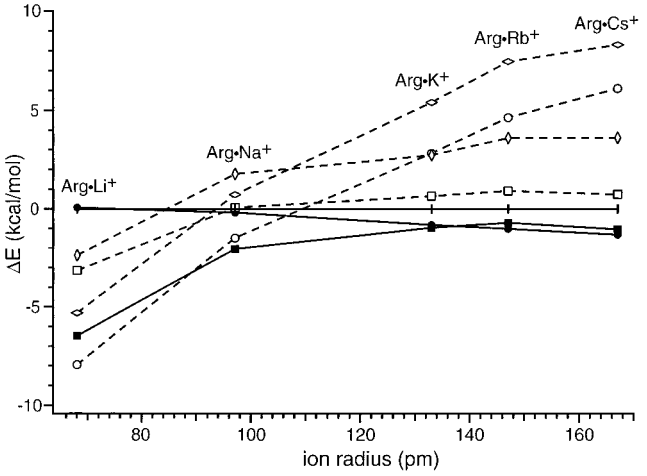


**Figure 5.** Relative energies of the seven structures for each Arg·$M^+$ calculated at the B3LYP/LACVP** level of theory. The energy of SB1 (+) is taken as the zero energy for each M. The other salt-bridge structures are SB2 (●) and SB3 (■). Salt-bridge structures are connected by solid lines. The charge-solvated structures are ChS1 (○), ChS2 (□), ChS3 (◇), and ChS4 (◊) and are connected by dashed lines.

structures. In all cases, the zero-point energy of the charge-solvated structure is lower by ~0.4 kcal/mol (Table 2). However, at the RHF/6-31+G* level, the reverse was found for Arg·$Li^+$ and Arg·$Na^+$, the only complexes for which this calculation was done. The zero-point energy for the charge-solvated structure is higher than that of the salt-bridge by 0.5 and 0.6 kcal/mol, respectively (Table 2). Because of this discrepancy and the cost of doing frequency calculations with the larger basis set, zero-point energies are listed in Table 2, but these values are not included in the reported energy differences between structures.

**TABLE 2: Difference in the Zero-Point Energy between the Lowest Energy Charge-Solvated and Salt-Bridge Structures of Arg·$M^+$**

| | Δ*E* (kcal/mol) | |
|---|---|---|
| M | RHF/3-21G | RHF/6-31+G* |
| Li | −0.4 | +0.5 |
| Na | −0.5 | +0.6 |
| K | −0.2 | |
| Rb | −0.3 | |

The basis set was increased with the addition of diffuse functions, and single-point energies were calculated at the B3LYP/LACVP++** level. The difference in energies between the most stable charge-solvated complex and most stable salt-bridge structure for each M is shown in Figure 6, and these values are reported in Table 3. The relative stability of the charge-solvated structure decreases with increasing metal ion size. The lowest energy charge-solvated conformer of Arg·$Li^+$ is more stable than the lowest energy salt-bridge conformer by 0.7 kcal/mol. For Arg·$Na^+$, the relative stabilities of the most stable salt-bridge and the lowest energy charge-solvated conformer reverse; the salt-bridge structure is favored by 0.7 kcal/mol. This energy difference increases to 3.2 kcal/mol for Arg·$K^+$. The difference then remains about the same and is calculated to be 3.7 and 3.2 kcal/mol for Arg·$Rb^+$ and Arg·$Cs^+$, respectively. The trends seen in these calculations are

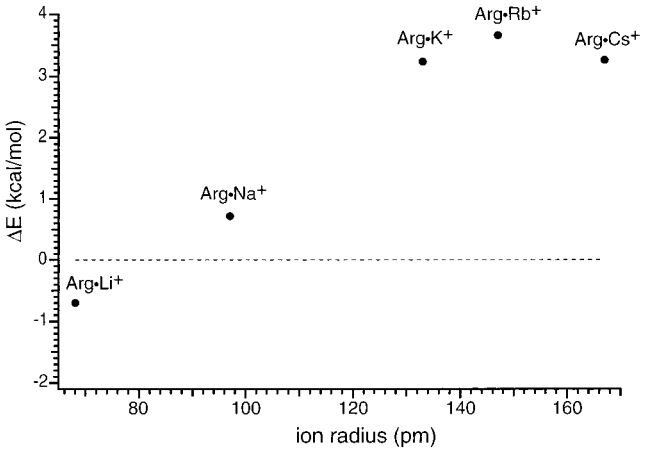


**Figure 6.** Energy difference between the most stable charge-solvated structure and the most stable salt-bridge structure at the B3LYP/LACVP++** level of theory as a function of metal ion size.

**TABLE 3: Effect of Basis Set on the Difference in Energy between the Lowest Energy Charge-Solvated and Salt-Bridge Conformers of Arg·M$^+$ [d]**

| | $\Delta E$ (kcal/mol) | | | | |
|---|---|---|---|---|---|
| M | LACVP** | LACVP++** | 6-31G** | 6-311G** | 6-311G++** |
| Li | −1.5[a] | −0.7 | −1.5[a] | | −0.1[a] |
| Na | 0.6[a] | 0.7 | 0.6[a] | | 1.3[a] |
| K | 1.6[a] | 3.2 | 3.4[b,c] | 4.1[b,c] | *b* |
| Rb | 1.9[a] | 3.7 | *b* | *b* | *b* |
| Cs | 2.1[a] | 3.3 | *b* | *b* | *b* |

[a] Geometry optimized at this level. [b] Basis set not available for M in the Jaguar v3.5 package. [c] Calculation done using Gaussian 92/DFT. [d] Values correspond to the differences in B3LYP single-point energy calculated from the B3LYP/LACVP** geometry unless otherwise noted and do not include a zero-point correction.

consistent with the gas-phase structure of the Arg·M$^+$ complex changing from a charge-solvated complex with the small metal ions to a salt-bridge structure with the large cations.

It should be noted that these calculations (with zero-point energies) reflect 0 K structures. The internal energy of the ions in the BIRD experiment correspond to temperatures of roughly 550−580 K. In the SORI−CAD experiment, the internal energy is slightly higher. Thus, the calculations and the experiment are not directly comparable due to the difference in internal energy. The charge-solvated form may be entropically favored; there are more structures of similar low energy for the charge-solvated vs salt-bridge form. This would favor the charge-solvated structure under the conditions of the experiment and may explain the difference in crossover point observed by experiment vs that calculated at 0 K.

**Effect of Basis Set.** Additional energy calculations on the lowest energy salt-bridge and charge-solvated B3LYP/LACVP** optimized structures of Arg·M$^+$ for M = Li, Na, and K were performed to investigate the effect of basis set (Table 3). The inclusion of additional valence functions to describe Arg·Li$^+$ and Arg·Na$^+$ resulted in a small increase (0.6 kcal/mol) in the stability of the salt-bridge structures over the charge-solvated structures; at the 6-311G++** level, the geometry optimized charge-solvated Arg·Li$^+$ is more stable than the salt-bridge structure by 0.1 kcal/mol compared to 0.7 kcal/mol at the LACVP++** level (equivalent to the 6-31G++** level for these ions). At this level, the salt-bridge structure of Arg·Na$^+$ is favored over the charge-solvated structure by 1.3 kcal/mol.

Replacing the effective core potential on K of the LACVP** basis with the 6-31G** basis increases the calculated stability of the salt-bridge structure from 1.6 to 3.4 kcal/mol. Using the triple-$\zeta$ 6-311G** basis set, this difference further increases to 4.1 kcal/mol. The latter two calculations were done using the GAUSSIAN 92/DFT program.

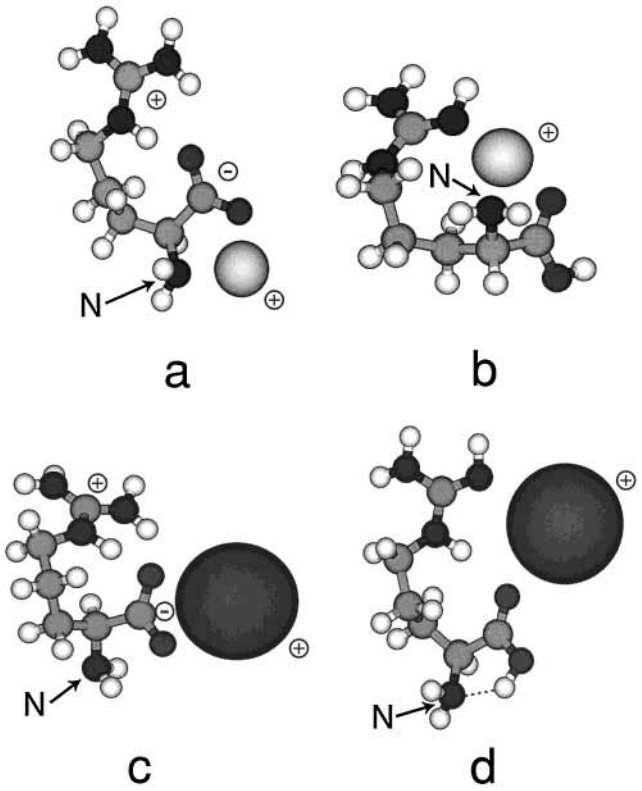


**Figure 7.** Geometry optimized structures for the lowest energy (a) salt-bridge and (b) charge-solvated structures of Arg·Li$^+$ and (c) salt-bridge and (d) charge-solvated structures of Arg·Cs$^+$. Structure b is more stable than structure a by 0.7 kcal/mol. Structure c is more stable than structure d by 3.3 kcal/mol.

These calculations indicate that with increasing the basis set, the trends in stability are maintained. It appears that the use of the effective core potential may lead to an underestimation of the relative stability of the salt-bridge structure of complexes for which it is used (M = K, Rb, Cs). However, even at a high level of theory (6-311G++**), the charge-solvated structure is marginally more stable than the salt-bridge structure for Arg·Li$^+$. Electron correlation may help to stabilize the charge-solvated compared to the salt-bridge structures. MP2/6-31G+* calculations indicate that the charge-solvated structure of Arg·Li$^+$ is more stable than the lowest energy salt-bridge structure by 3.2 kcal/mol.

The calculated energy difference between these isomers is small. Nevertheless, the similar results obtained with larger basis sets provide an additional indication that the salt-bridge structure is favored for the larger alkali ions.

**Low-Energy Structures.** Figure 7 shows the lowest energy salt-bridge and charge-solvated conformers found for Arg·Li$^+$ and Arg·Cs$^+$. For Arg·Li$^+$, these are SB3 and ChS1. For Arg·Cs$^+$, these are SB2 and ChS2. In the lowest energy salt-bridge structure of Arg·Li$^+$ (Figure 7a), the Li$^+$ is stabilized through interactions with the N-terminus and one oxygen of the C-terminal carboxylate of the Arg. The structure is further stabilized by a hydrogen bond between the other carboxylate oxgygen and the protonated side chain. In the most stable charge-solvated structure of Arg·Li$^+$ (Figure 7b), the arginine surrounds the Li$^+$ and solvates the charge through multiple interactions with the N-terminus, the carbonyl oxygen, and a

terminal nitrogen of the side chain. In contrast, the much larger $Cs^+$ ion cannot fit inside a pocket formed by the arginine (parts c and d of Figure 7). In the lowest energy charge-solvated structure of Arg·$Cs^+$ (Figure 7d), the $Cs^+$ only superficially fits within the pocket formed by the Arg; the $Cs^+$ sits on the side of the Arg and solvation is not nearly as effective as it is for Arg·$Li^+$. Although a hydrogen bond between the N-terminus and the acidic hydrogen of the C-terminus helps stabilize this structure, it is higher in energy than the salt-bridge structure by 3.3 kcal/mol. In the lowest energy salt-bridge structure, the $Cs^+$ interacts with both oxygens of the carboxylate. A hydrogen bond between the guanidino group and carboxylate lends additional stability to the structure. The Arg·$Cs^+$ of the SB3 family (not shown) is only 0.3 kcal/mol higher in energy than SB2 at the LACVP** level of theory.

## Conclusions

Results from both experiment and theory indicate that the structure of gas-phase arginine−alkali metal complexes changes as the size of the metal ion increases. For the smaller metal ions, the neutral arginine solvates the metal ion. For the larger metal ions, a salt bridge is formed in which the arginine exists as a zwitterion (side chain protonated, C-terminus deprotatoned). DFT calculations at the B3LYP/LACVP++** level indicate that the salt-bridge form of these ions becomes progressively more stable relative to the charge-solvated form with increasing cation size. For Arg·$Li^+$, the charge-solvated form is 0.7 kcal/mol more stable. For Arg·$Na^+$, the salt-bridge form is 0.7 kcal/mol more stable. For Arg·$M^+$, M = K, Rb and Cs, the salt-bridge structure is 3.2−3.7 kcal/mol more stable.

These calculations are in good agreement with the observed unimolecular dissociation pathways of these ions. The primary dissociation product under low-energy conditions changes from loss of $H_2O$ for H, Li, and Na to loss of $NH_3$ for K, Rb, and Cs. The loss of water can only come from a charge-solvated ion, whereas loss of $NH_3$ can readily occur from the protonated side chain of arginine, consistent with a salt-bridge structure. Loss of $NH_3$ is observed for *N*,*N*-dimethyl arginine·$M^+$ with M = H, Na, K, Rb, and Cs, indicating that loss of $NH_3$ can originate from the guanidine group of the side chain in this ion. Dissociation of cationized methyl esters of arginine results in the loss of $CH_3OH$ and $M^+$ (for larger M); loss of $NH_3$ is observed only from the protonated species. The methyl ester cannot form a salt bridge. The higher thermal stability of the methyl ester form of Arg·$K^+$ indicates that loss of $CH_3OH$ is not an intrinsically low-energy process but rather the pathway for loss of $NH_3$ has been shut down in the metalated arginine methyl esters. Dissociation of N-acetylated arginine complexes results in loss of $H_2O$ for all metal ions with no loss of $NH_3$ observed. The additional carbonyl group on the N-terminus of acetylated arginine results in increased charge-solvating ability, stabilizing the charge-solvated form.

Although the dissociation experiments provide indirect evidence of the isomeric structure of these ions, the experimentally observed dissociation pathways are in good agreement with the relative stabilities of these ions calculated using density functional theory. Taken together, both the experiments and theory provide strong support for the change in structure of Arg·$M^+$ from a charge-solvated ion to a salt-bridge structure with increasing alkali metal ion size.

**Acknowledgment.** The authors are grateful for generous financial support provided by the National Science Foundation (CHE-9726183) and the National Institutes of Health (IR29GM50336-01A2).

## References and Notes

(1) Jensen, J. H.; Gordon, M. S. *J. Am. Chem. Soc.* **1991**, *113*, 7917−7924.
(2) Hu, C. H.; Shen, M.; Schaefer, H. F., III *J. Am. Chem. Soc.* **1993**, *115*, 2923−2928.
(3) Ding, Y. B.; Krogh-Jespersen, K. *Chem. Phys. Lett.* **1992**, *199*, 261−266.
(4) Csaszar, A. G. *J. Am. Chem. Soc.* **1992**, *114*, 9568−9575.
(5) Ding, Y.; Krogh-Jespersen, K. *J. Comput. Chem.* **1996**, *17*, 338−349.
(6) Jensen, J. H.; Gordon, M. S. *J. Am. Chem. Soc.* **1995**, *117*, 8159−8170.
(7) Jensen, F. *J. Am. Chem. Soc.* **1992**, *114*, 9533−9537.
(8) Hoyau, S.; Ohanessian, G. *Chem.−Eur. J.* **1998**, *4*, 1561−1569.
(9) Suenram, R. D.; Lovas, F. J. *J. Mol. Spectrosc.* **1978**, *72*, 372−382.
(10) Locke, M. J.; McIver, R. T., Jr. *J. Am. Chem. Soc.* **1983**, *105*, 4226−4232.
(11) Iijima, K.; Tanaka, K.; Onuma, S. *J. Mol. Struct.* **1991**, *246*, 257−266.
(12) Price, W. D.; Jockusch, R. A.; Williams, E. R. *J. Am. Chem. Soc.* **1997**, *119*, 11988−11989.
(13) Chapo, C. J.; Paul, J. B.; Provencal, R. A.; Roth, K.; Saykally, R. J. *J. Am. Chem. Soc.* **1998**, *120*, 12956−12957.
(14) Wyttenbach, T.; Bushnell, J. E.; Bowers, M. T. *J. Am. Chem. Soc.* **1998**, *120*, 5098−5103.
(15) Beauchamp, J. L.; Lee, S.-W.; Marzluff, E. Presented at the 45th ASMS Conference, Palm Springs, CA, June 1−5, 1997.
(16) Rizzo, T. R.; Park, Y. D.; Levy, D. H. *J. Chem. Phys.* **1986**, *85*, 6945−6951.
(17) Schnier, P. D.; Price, W. D.; Jockusch, R. A.; Williams, E. R. *J. Am. Chem. Soc.* **1996**, *118*, 7178−7189.
(18) Price, W. D.; Schnier, P. D.; Jockusch, R. A.; Strittmatter, E. F.; Williams, E. R. *J. Am. Chem. Soc.* **1996**, *118*, 10640−10644.
(19) Jockusch, R. A.; Schnier, P. D.; Price, W. D.; Strittmatter, E. F.; Demirev, P. A.; Williams, E. R. *Anal. Chem.* **1997**, *69*, 1119−1126.
(20) Yu, W.; Vath, J. E.; Huberty, M. C.; Martin, S. A. *Anal. Chem.* **1993**, *65*, 3015−3023.
(21) Qin, J.; Chait, B. T. *J. Am. Chem. Soc.* **1995**, *117*, 5411−5412.
(22) Lee, S. W.; Kim, H. S.; Beauchamp, J. L. *J. Am. Chem. Soc.* **1998**, *120*, 3188−3195.
(23) Tang, X. J.; Thibault, P.; Boyd, R. K. *Org. Mass Spectrom.* **1993**, *28*, 1047−1052.
(24) Grese, R. P.; Cerny, R. L.; Gross, M. L. *J. Am. Chem. Soc.* **1989**, *111*, 2835−2842.
(25) Deery, M. J.; Summerfield, S. G.; Buzy, A.; Jennings, K. R. *J. Am. Soc. Mass Spectrom.* **1997**, *8*, 253−261.
(26) Campbell, S.; Rodgers, M. T.; Marzluff, E. M.; Beauchamp, J. L. *J. Am. Chem. Soc.* **1995**, *117*, 12840−12854.
(27) Cox, K. A.; Gaskell, S. J.; Morris, M.; Whiting, A. *J. Am. Soc. Mass Spectrom.* **1996**, *7*, 522−531.
(28) Summerfield, S. G.; Whiting, A.; Gaskell, S. J. *Int. J. Mass Spectrom. Ion Processes* **1997**, *162*, 149−161.
(29) Gonzalez, J.; Besada, V.; Garay, H.; Reyes, O.; Padron, G.; Tambara, Y.; Takao, T.; Shimonishi, Y. *J. Mass Spectrom.* **1996**, *31*, 150−158.
(30) Wyttenbach, T.; Witt, M.; Bowers, M. T. *Int. J. Mass Spectrom.* **1999**, *183*, 243−252.
(31) Price, W. D.; Schnier, P. D.; Williams, E. R. *Anal. Chem.* **1996**, *68*, 859−866.
(32) Hay, P. J.; Wadt, W. R. *J. Chem. Phys.* **1985**, *82*, 270−283.
(33) Hehre, W. J.; Radom, L.; Schleyer, P. R.; Pople, J. A. *Ab initio Molecular Orbital Theory*; Wiley: New York, 1986.
(34) The gas-phase basicity of the amino acids glycine, alanine, valine, leucine, and isoleucine are 204−211 kcal/mol compared to 227 kcal/mol for guanidine, the functional group of the arginine side chain. Values from: Hunter, E. P.; Lias, S. G. In *NIST Chemistry WebBook, NIST Standard Reference Database Number 69*; Mallard, W. G., Linstrom, P. J., Eds.; National Institute of Standards and Technology: Gaithersburg, MD, November 1998 (release, http://webbook.nist.gov).